Journal of Molecular Structure 1012 (2012) 22–30

Contents lists available at SciVerse ScienceDirect

Journal of Molecular Structure

journal homepage: www.elsevier.com/locate/molstruc

FT-IR, FT-Raman, surface enhanced Raman scattering and computational study of 2-(p-fluorobenzyl)-6-nitrobenzoxazole

Y. Sheena Mary [a,b,*], K. Raju [b], Tugba Ertan Bolelli [c], Ilkay Yildiz [c], Helena I.S. Nogueira [d], Carlos M. Granadeiro [d], Christian Van Alseony [e]

[a] Department of Physics, Fatima Mata National College, Kollam, Kerala, India
[b] Department of Physics, University College, Trivandrum, Kerala, India
[c] Faculty of Pharmacy, Department of Pharmaceutical Chemistry, Ankara University, Tandogan 06100, Ankara, Turkey
[d] Department of Chemistry, CICECO, University of Aveiro, 3810-193 Aveiro, Portugal
[e] Department of Chemistry, University of Antwerp, B2610 Antwerp, Belgium

ARTICLE INFO

Article history:
Received 21 November 2011
Received in revised form 26 December 2011
Accepted 27 December 2011
Available online 4 January 2012

Keywords:
FT-IR
FT-Raman
SERS
DFT
Benzoxazole

ABSTRACT

FT-IR and FT-Raman spectra of 2-(p-fluorobenzyl)-6-nitrobenzoxazole were recorded and analyzed. A surface enhanced Raman scattering spectrum (SERS) was recorded in silver colloid. Using Gaussian03 set of quantum chemistry codes, the vibrational wavenumbers and corresponding vibrational assignments were examined theoretically. The presence of CH_2 and NO_2 bands in the SERS spectrum indicates the nearness of these groups to the metal surface, which affects the orientation and metal molecule interaction. From the SERS study, it is inferred that the para substituted phenyl ring is more tilted while the tri-substituted phenyl ring assumes a nearly perpendicular orientation with respect to the metal surface. The results indicate that the B3LYP method is able to provide satisfactory results for predicting vibrational wavenumbers and structural parameters. The calculated first hyperpolarizability is comparable with the reported values of similar derivatives. The geometrical parameters of the title compound are in agreement with that of similar derivatives.

1. Introduction

Benzoxazoles have been studied by researchers for many years because they constitute an important class of heterocyclic compounds exhibiting substantial chemotherapeutic activities [1–5]. Heterocyclic molecules with acid and basic groups, such as 2-(2-hydroxyphenyl)benzoxazole and its derivatives [6] often give rise to proton-transfer process in which the proton can be interchanged between the two groups or between these groups and the surrounding media [7,8]. Derivatives of benzoxazole, benzimidazoles and related fused heterocyclic compounds exhibit significant in vitro antimicrobial and antiviral activities [9,10]. Bigotto and Pergolese reported the surface enhanced Raman spectroscopic studies of 2-mercaptobenzoxazole on silver sols [11]. Liquid crystals containing heterocycles such as 1,3,4-oxadiazole [12], 1,2,3-triazole [13], and benzoxazole [14], have recently been explored in the design and synthesis of novel molecular functional materials, where liquid crystalline phases, geometry, polarity, luminescence and other properties may be varied by introducing heteroatoms [15]. Tasal et al. [16] reported the molecular structure, vibrational frequencies and infrared intensities of a benzoxazole derived in the ground state by HF and DFT methods. In the present work, the IR, Raman, SERS and theoretical calculations of the wavenumbers for the title compound are reported. Nonlinear optics deals with the interaction of applied electromagnetic fields in various materials to generate new electromagnetic fields, altered in wavenumber, phase or other physical properties [17]. Organic molecules enable to manipulate photonic signals efficiently and are of importance in technologies such as optical communication, optical computing and dynamic image processing [18,19]. Phenyl substituents can increase molecular hyperpolarizability [20,21]. Many organic molecules, containing conjugated π electrons and characterized by large values of molecular first hyperpolarizabilities, were analyzed by means of vibrational spectroscopy [22]. In this context, the hyperpolarizability of the title compound is calculated in the present study.

2. Experimental

The chemicals were purchased from the commercial venders and were used without purification. The title compound was prepared by the protocol reported by Ertan et al. [23] and the general procedure is as follows: The derivatives were synthesized by

* Corresponding author at: Department of Physics, Fatima Mata National College, Kollam, Kerala, India. Tel.: +91 9895471621.
E-mail address: ysheena@rediffmail.com (Y. Sheena Mary).

0022-2860/$ - see front matter © 2012 Elsevier B.V. All rights reserved.
doi:10.1016/j.molstruc.2011.12.042

heating 0.01 mol appropriate o-aminophenol with 0.01 mol suitable acid in 24 g polyphosphoric acid and stirring for 2–3 h. At the end of the reaction period, the residue was poured into an ice water mixture and neutralized with an excess of 10 M NaOH solution extracted with ethyl acetate. Then, this solution was dried over anhydrous sodium sulphate and evaporated under diminished pressure. The residue was boiled with 200 mg charcoal and filtered. After the evaporation of solvent in vacuo, the crude product was obtained and re-crystallized from ethanol. The reactions were monitored and the purity of the products was checked by thin layer chromatography (TLC). Silica gel 60 F_{254} chromatoplates were used for TLC. All the melting points were measured with a capillary melting point apparatus (Buchi SMP 20 and Electrothermal 9100). Yield was calculated after re-crystallization. The ^{1}H NMR spectrum was recorded employing a VARIAN Mercury 400 MHz FT spectrometer, chemical shifts (δ) are in parts per million relative to TMS, and coupling constants (J) are reported in hertz. Elemental analysis was taken on a Leco 932 CHNS-O analyzer. The results of the elemental analysis (C, H, N) was within ±0.4% of the calculated amount. Yield: 60%, mp 109–110 °C. ^{1}H NMR (400 MHz, $CDCl_3$): δ 4.31 (s, 2H), 7.06 (m, 2H), 7.37 (m, 2H), 7.77 (dd, 1H, J 8.8, 1.2 Hz), 8.27 (m, 1H), 8.39 (d, 1H, J 1.6 Hz). Anal. Found: C, 61.19; H, 3.20; N, 10.18; Calcd for $C_{14}H_9N_2O_3F$: C, 61.77; H, 3.33; N, 10.29. The IR spectrum (Fig. 1) was recorded on a Jasco FTIR-420 spectrometer with the sample in standard KBr pellet technique. The spectral resolution was 2 cm^{-1}. The FT-Raman spectra (Figs. 2 and 3) were obtained on a Bruker RFS 100/S, Germany. For excitation of the spectrum, the emission of a Nd:YAG laser was used, excitation wavelength 1064 nm, maximal power 150 mW, measurement on solid sample, spectral resolution 2 cm^{-1}. The aqueous silver colloid used in the SERS experiment was prepared by reduction of silver nitrate by sodium citrate, using the Lee–Meisel method [24]. Solutions of the title compound were made up in ethanol (0.1 mmol in 1 cm^3 of solvent) and transferred by a micro syringe into the silver colloid (10 μL in 1 cm^3 of colloid) such that the overall concentration was 10^{-3} mol dm^{-3}. Colloid aggregation was induced by addition of an aqueous solution of $MgCl_2$ (one drop of a 2 mol dm^{-3} solution). Polyvinylpyrrolidone was then used to stabilize the colloid (one drop of 0.1 g/10 cm^3 aqueous solution). The final colloid mixture was placed in a glass tube and the Raman spectrum registered.

3. Computational details

The vibrational wavenumbers were calculated using the Gaussian03 software package on a personal computer [25]. The computations were performed at HF/6-31G* and B3LYP/6-31G* levels of theory to get the optimized geometry (Fig. 4) and vibrational wavenumbers of the normal modes of the title compound. Parameters corresponding to the optimized geometry of the title compound are given in Table 1. The DFT partitions, the electronic energy $E = E_T + E_V + E_J + E_{XC}$, where E_T, E_V and E_J are electronic kinetic energy, electron nuclear attraction and electron–electron repulsion terms, respectively. The electron correlation is taken into account in the DFT via the exchange–correlation term E_{XC}, which includes exchange energy arising from the anti-symmetry of quantum mechanical wave function and dynamic correlation in the motion of individual electron, and it makes DFT dominant over conventional HF procedure [26]. DFT calculations were carried out with Becke's three-parameter hybrid model using the Lee–Yang–Parr correlation functional (B3LYP) method. Molecular geometries were fully optimized by Berny's optimization algorithm using redundant internal coordinates. Harmonic vibrational wavenumbers were calculated using analytic second derivatives to confirm the convergence to minima in the potential surface. At the optimized structure of the examined species, no imaginary wavenumber modes were obtained, proving that a true minimum on the potential surface was found. The optimum geometry was determined by minimizing the energy with respect to all geometrical parameters without imposing molecular symmetry constraints. The DFT hybrid B3LYP functional tends also to overestimate the fundamental modes: therefore scaling factors have to be used for obtaining a considerably better agreement with experimental data [27]. Scaling factors 0.9613 and 0.8929 have been uniformly applied for the DFT and HF calculated wavenumbers [26]. The observed disagreement between theory and experiment could be a consequence of the anharmonicity and of the general tendency of the quantum chemical methods to overestimate the force constants at the exact equilibrium geometry [28]. Potential energy surface scan studies have been carried out to understand the stability of planar and non-planar structures of the molecule. The profiles of potential energy surface for torsion angles C_{15}—N_{14}—C_3—C_2,

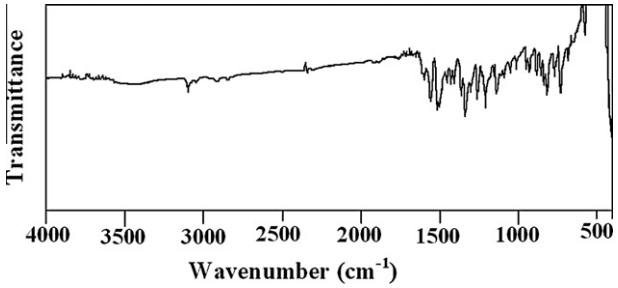

Fig. 1. IR spectrum of 2-(p-fluorobenzyl)-6-nitrobenzoxazole.

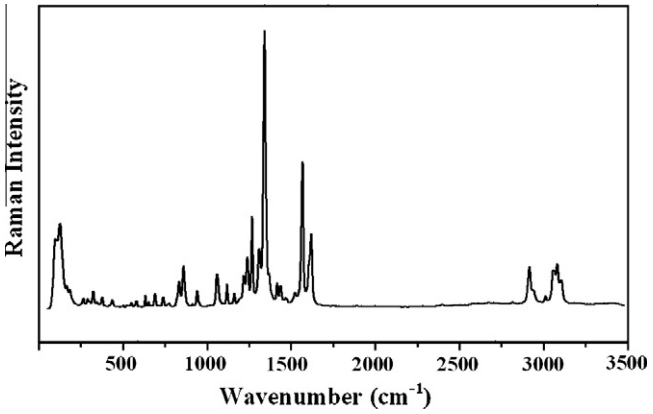

Fig. 2. Raman spectrum of 2-(p-fluorobenzyl)-6-nitrobenzoxazole.

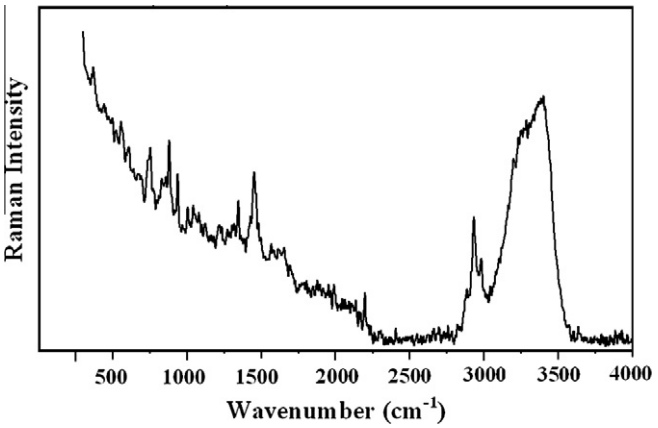

Fig. 3. SERS spectrum of 2-(p-fluorobenzyl)-6-nitrobenzoxazole.

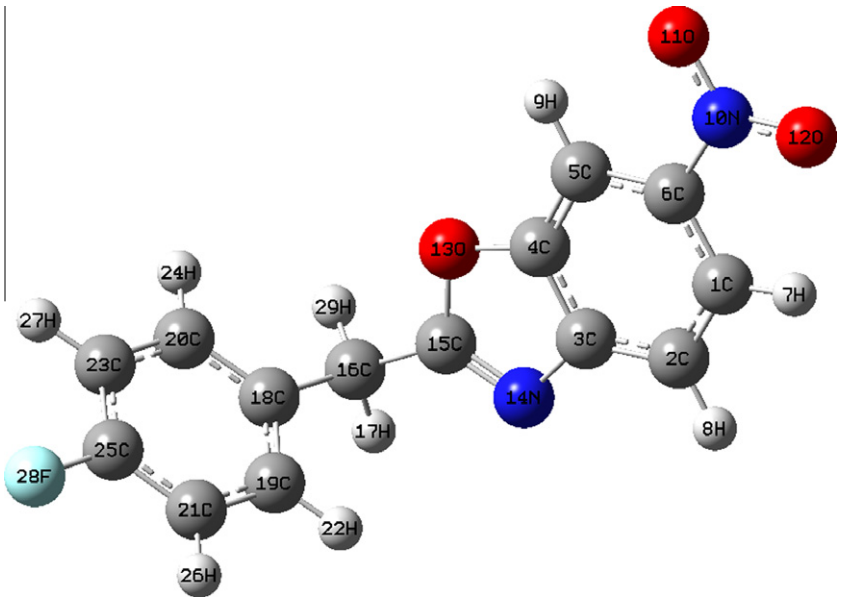

Fig. 4. Optimized geometry (B3LYP) of 2-(p-fluorobenzyl)-6-nitrobenzoxazole.

C_{16}—C_{15}—N_{14}—C_3, C_{19}—C_{18}—C_{16}—C_{15} and C_{20}—C_{18}—C_{16}—C_{15} are computed. The energy is minimum for −179.8° (−973.825), −177.6° (−973.82559), −65.7° (−973.82458) and 114.6° (−973.82467 Hartree), respectively for the above torsion angles. The potential energy distribution (PED) was calculated with the help of GAR2PED software package [29].

4. Results and discussion

The observed IR and Raman bands and calculated (scaled) wavenumbers and assignments are given in Table 2.

4.1. IR and Raman spectra

In nitro compounds, $\upsilon_{as}NO_2$ are located in the region 1580 ± 80 cm^{-1}. The nitro benzene derivatives show $\upsilon_{as}NO_2$ in the region 1535 ± 30 cm^{-1} and the 3-nitropyridine at 1530 ± 20 cm^{-1} [30]. In the present case, $\upsilon_{as}NO_2$ are obtained at 1429 theoretically (DFT) and at 1435 cm^{-1} in both IR and Raman spectra. In nitro compounds, υ_sNO_2 are located in the region 1300–1360 cm^{-1}. The nitrobenzene derivatives show υ_sNO_2 in 1345 ± 30 cm^{-1} and the 3-nitropyridines in 1350 ± 20 cm^{-1}. For the title compound, υ_sNO_2 is observed at 1363 cm^{-1} (DFT), 1368 cm^{-1} (IR) and 1367 cm^{-1} (Raman). In the aromatic nitro compounds, bands are usually seen at 855 ± 40 cm^{-1} (NO_2 scissors deformation δNO_2), 760 ± 30 cm^{-1} (NO_2 out of plane wag ωNO_2), 540 ± 30 cm^{-1} (NO_2 in-plane rock ρNO_2) and 70 ± 20 cm^{-1} (τNO_2). In the present case, the observed values for δNO_2 are 778 (DFT), 773 (IR) and 773 cm^{-1} (Raman); γNO_2 is 692 cm^{-1} (DFT); δNO_2 are 533 (DFT), 522 (IR) and 528 cm^{-1} (Raman) and τNO_2 is at 61 cm^{-1} (DFT). Panicker et al. [31] reported the NO_2 deformation bands at 800, 724, 534 cm^{-1} (theoretically) and 809, 727, 717, 524 cm^{-1} (experimentally). Sundaraganesan et al. [32] reported the NO_2 deformation bands at 839, 744 and 398 cm^{-1} experimentally and 812, 716, 703 and 327 cm^{-1} theoretically.

The vibrations of the CH_2 group fall in the range 2940 ± 20 cm^{-1}, 2855 ± 45 cm^{-1}, 1440 ± 10 cm^{-1}, 1340 ± 25 cm^{-1}, 1260 ± 10 cm^{-1} and 800 ± 25 cm^{-1} [30]. In the present case, $\upsilon_{as}CH_2$ is found at 3009 (DFT) and 3011 cm^{-1} (Raman), υ_sCH_2, δCH_2, ωCH_2, τCH_2 and ρCH_2 at 2959 (DFT), 2918 cm^{-1} (Raman); 1456 cm^{-1} (DFT); 1335 (DFT), 1344 (IR) and 1341 (Raman) cm^{-1}; 1250 (DFT) and 764 (DFT), 763 (Raman) cm^{-1}.

Fluorine atoms directly attached to an aromatic ring give rise to bands in the region 1270–1100 cm^{-1} [33]. Many of these compounds, including compounds with one fluorine on the ring, absorb near 1230 cm^{-1} [33]. The υCF is reported at 1233 (IR) and 1244 cm^{-1} (HF) [34] and at 1227 (IR) and 1239 cm^{-1} (HF) [35] for fluoro-phenyl compounds. In the present case, it is obtained at 1214 (IR), 1216 (Raman) and 1218 cm^{-1} (DFT).

Due to the stretching of the phenyl carbon–nitrogen bond, primary aromatic amines with the nitrogen directly on the ring absorb strongly at 1330–1260 cm^{-1} [33]. For the title compound, υC_6N_{10} is observed at 1233 (DFT) and 1238 cm^{-1} (Raman) υC_3N_{14} at 1209 (DFT) and 1194 cm^{-1} (Raman). Mary et al. [35] reported υCN at 1343 (IR) and 1312 cm^{-1} theoretically. Ambujakshan et al. [36] reported υCN mode at 1331, 1279 (IR) and 1323, 1273 cm^{-1} theoretically. The C=N stretching skeletal bands are obtained in the range 1672–1566 cm^{-1} [37–40]. Saxena et al. [38] reported this value at 1608 cm^{-1}, Klots and Collier [41] at 1517 cm^{-1} and Anto et al. [34] as 1643 cm^{-1} theoretically, 1661 cm^{-1} (Raman) and 1671 cm^{-1} (IR). In the present case, υC_{15}=N_{14} is observed at 1536 (DFT), 1523 (IR) and 1522 (Raman) cm^{-1}.

Since the identification of all the normal modes of vibration of large molecules is not trivial, we tried to simplify the problem by considering each molecule as substituted benzene. Such an idea has already been successfully utilized by several workers for vibrational assignments of molecules containing multiple homo and hetero aromatic rings [34,42–46]. In the present case, the para-substituted ring (1,4-diheavy substituted phenyl ring), 1,2,4-triheavy substituted phenyl ring and benzoxazole ring are designated as PhI, PhII and Ring III respectively. The υCH vibrations are usually expected in the range 3020–3120 cm^{-1} [30]. For RingI, the υCH vibrations are observed at 3120, 3119, 3085 and 3084 theoretically; at 3106 (IR) and 3104 cm^{-1} (Raman) experimentally. For RingII, the υCH modes fall in the range 3000–3110 cm^{-1} [30]. The DFT calculations give the three expected υCH modes at 3155, 3142 and 3122 cm^{-1} with a PED prediction of 99% contribution. The υPh modes are expected in the regions 1280–1630 cm^{-1} and 1260–1640 cm^{-1} respectively for ring I and ring II [37]. The υPhI modes are observed at 1605, 1566, 1511, 1416, 1308 cm^{-1} in the IR spectrum; at 1566, 1415, 1309 cm^{-1} in the Raman spectrum and at

Table 1
Geometrical parameters of (B3LYP) the title compound.

Bond lengths (Å)		Bond angles (°)		Dihedral angles (°)	
C_1—C_2	1.3943	A(2,1,6)	120.2	D(6,1,2,3)	−0.1
C_1—C_6	1.4083	A(2,1,7)	121.3	D(6,1,2,8)	179.9
C_1—H_7	1.0814	A(6,1,7)	118.5	D(7,1,2,3)	179.9
C_2—C_3	1.3978	A(1,2,3)	117.6	D(7,1,2,8)	−0.1
C_2—H_8	1.0825	A(1,2,8)	121.5	D(2,1,6,5)	0.0
C_3—C_4	1.4091	A(3,2,8)	120.9	D(2,1,6,10)	−179.9
C_3—N_{14}	1.4113	A(2,3,4)	120.2	D(7,1,6,5)	−180.0
C_4—C_5	1.3814	A(2,3,14)	130.9	D(7,1,6,10)	0.0
C_4—O_{13}	1.3990	A(4,3,14)	108.9	D(1,2,3,4)	0.0
C_5—C_6	1.4003	A(3,4,5)	123.9	D(1,2,3,14)	179.8
C_5—H_9	1.0803	A(3,4,13)	107.4	D(8,2,3,4)	−180.0
C_6—N_{10}	1.4644	A(5,4,13)	128.7	D(8,2,3,14)	−0.2
N_{10}—O_{11}	1.2653	A(4,5,6)	114.5	D(2,3,4,5)	0.1
N_{10}—O_{12}	1.2645	A(4,5,9)	124.1	D(2,3,4,13)	179.9
C_{15}—O_{13}	1.4186	A(6,5,9)	121.4	D(14,3,4,5)	−179.8
C_{15}—N_{14}	1.3081	A(1,6,5)	123.6	D(14,3,4,13)	−0.0
C_{15}—C_{16}	1.4876	A(1,6,10)	118.5	D(2,3,14,15)	−179.8
C_{16}—H_{17}	1.0945	A(5,6,10)	117.9	D(4,3,14,15)	0.0
C_{16}—C_{18}	1.5276	A(6,10,11)	118.0	D(3,4,5,6)	−0.1
C_{16}—H_{29}	1.0946	A(6,10,12)	118.2	D(3,4,5,9)	179.9
C_{18}—C_{19}	1.4057	A(11,10,12)	123.8	D(13,4,5,6)	−179.8
C_{18}—C_{20}	1.4026	A(4,13,15)	104.1	D(13,4,5,9)	0.2
C_{19}—C_{21}	1.3970	A(3,14,15)	105.7	D(3,4,13,15)	−0.0
C_{19}—H_{22}	1.0856	A(13,15,14)	113.8	D(5,4,13,15)	179.7
C_{20}—C_{23}	1.3993	A(13,15,16)	117.0	D(4,5,6,1)	0.1
C_{20}—H_{24}	1.0854	A(14,15,16)	129.1	D(4,5,6,10)	−180.0
C_{21}—C_{25}	1.3918	A(15,16,17)	107.1	D(9,5,6,1)	180.0
C_{21}—H_{26}	1.0830	A(15,16,18)	112.8	D(9,5,6,10)	−0.0
C_{23}—C_{25}	1.3897	A(15,16,29)	109.0	D(1,6,10,11)	179.9
C_{23}—H_{27}	1.0829	A(17,16,18)	110.3	D(1,6,10,12)	−0.1
C_{25}—F_{28}	1.3915	A(17,16,29)	107.8	D(5,6,10,11)	−0.1
		A(18,16,29)	109.7	D(5,6,10,12)	179.9x
		A(16,18,19)	120.1	D(4,13,15,14)	0.0
		A(16,18,20)	120.8	D(4,13,15,16)	177.9
		A(19,18,20)	119.2	D(3,14,15,13)	−0.0
		A(18,19,21)	120.7	D(3,14,15,16)	−177.6
		A(18,19,22)	119.6	D(13,15,16,17)	161.0
		A(21,19,22)	119.6	D(13,15,16,18)	−77.5
		A(18,20,23)	120.8	D(13,15,16,29)	44.6
		A(18,20,24)	119.8	D(14,15,16,17)	−21.5
		A(23,20,24)	119.4	D(14,15,16,18)	100.1
		A(19,21,25)	118.5	D(14,15,16,29)	−137.9
		A(19,21,26)	121.6	D(15,16,18,19)	−65.7
		A(25,21,26)	119.9	D(15,16,18,20)	114.6
		A(20,23,25)	118.4	D(17,16,18,19)	54.0
		A(20,23,27)	121.6	D(17,16,18,20)	−125.7
		A(25,23,27)	120.0	D(29,16,18,19)	172.7
		A(21,25,23)	122.5	D(29,16,18,20)	−7.1
		A(21,25,28)	118.7	D(16,18,19,21)	−179.9
		A(23,25,28)	118.8	D(16,18,19,22)	0.7
				D(20,18,19,21)	0.2
				D(20,18,19,22)	−179.5
				D(16,18,20,23)	179.5
				D(16,18,20,24)	−0.6
				D(19,18,20,23)	−0.3
				D(19,18,20,24)	179.7
				D(18,19,21,25)	−0.0
				D(18,19,21,26)	179.9
				D(22,19,21,25)	179.7
				D(22,19,21,26)	−0.4
				D(18,20,23,25)	0.2
				D(18,20,23,27)	−179.9
				D(24,20,23,25)	−179.8
				D(24,20,23,27)	0.1
				D(19,21,25,23)	−0.1
				D(19,21,25,28)	179.9
				D(26,21,25,23)	180.0
				D(26,21,25,28)	−0.0
				D(20,23,25,21)	0.0
				D(20,23,25,28)	−180.0
				D(27,23,25,21)	−179.9
				D(27,23,25,28)	0.1

1603, 1589, 1506, 1413, and 1310 cm^{-1} in the DFT calculations for ring I. The same is observed at 1659, 1463 cm^{-1} in the IR spectrum; at 1620, 1467 cm^{-1} in the Raman spectrum and at 1609, 1596, 1458, 1405, 1304 cm^{-1} theoretically for ring II. Due to the contributions from other modes, most of the vibrational modes are not pure. The ring breathing mode of the para-diheavy substituted benzene compounds with entirely different substituents has been reported in the interval 780–880 cm^{-1} [47]. In asymmetric trisubstituted benzene, when all the three substituents are light, the ring breathing mode falls in the range 500–600 cm^{-1}; when all the three substituents are heavy, it appears above 1100 cm^{-1} and in the case of mixed substituents, it falls in the range 600–750 cm^{-1} [46]. In the present case, the ring breathing mode is reported at 829 cm^{-1} in DFT and 832 cm^{-1} in Raman spectrum for ring I and at 1042 cm^{-1} in DFT, 1056 cm^{-1} in IR and 1057 in Raman for ringII. Panicker et al. [48] has reported the ring breathing mode for a para-disubstituted benzene compound at 873 cm^{-1} (IR) and at 861 cm^{-1} theoretically. Madhavan et al. [49] has reported the same for a compound having two tri-substituted benzene rings as 1110 cm^{-1} and 1083 cm^{-1}.

δCH in-plane deformation mode and γCH out-of-plane deformation mode for para-disubstituted benzene falls in the range 1305–995 cm^{-1} and 970–800 cm^{-1} respectively [30]. In the present case, δCH mode for ring I are observed at 1310, 1165, 1107, 1014 cm^{-1} (DFT); 1308, 1160, 1016 cm^{-1} (IR) and 1309 cm^{-1} (Raman). γCH mode for ring I are observed in the range 961–845 cm^{-1} (theoretically); 951, 934 cm^{-1} (IR) and at 940 cm^{-1} (Raman). δCH in-plane bending vibration for tri-substituted benzenes are expected in the region 1050–1290 cm^{-1} [30]. For the title compound, δCH modes for ring PhII are observed at 1261, 1121, 1093 cm^{-1} (DFT); 1266, 1095 cm^{-1} (IR) and 1266, 1118 cm^{-1} (Raman).

The γCH vibrations are mainly determined by the number of adjacent hydrogen atoms on the ring. Although strongly electron attracting substituent groups, such as nitro-, can result in an increase (about 30 cm^{-1}) in the frequency of the vibration, these vibrations are not very much affected by the nature of the substituents. 1,2,4-trisubstituted benzenes show a medium absorption at 940–840 cm^{-1} and a strong band at 780–760 cm^{-1}. In Raman spectra, the out of plane bands are usually weak [50]. In the present case, these vibrations are observed at 981, 913, 844 cm^{-1} (DFT) and 838 cm^{-1} in IR. The shift in the DFT values are due to the presence of nitro compounds as discussed above. The substituent sensitive modes and ring deformations are also identified and assigned (Table 2).

4.2. Geometrical parameters and first hyper polarizability

No X-ray crystallographic data of this molecule has yet been established to the best of our knowledge. However, the theoretical results obtained are almost comparable with the reported structural parameters of the parent molecules. Lifshitz et al. [51] reported the bond lengths for N_{14}—C_{15}, O_{13}—C_{15}, O_{13}—C_4, C_3—C_2, C_4—C_5, C_3—C_4, and N_{14}—C_3 as 1.291, 1.372, 1.374, 1.39, 1.4, 1.403 and 1.401 Å. The corresponding values in the present case are 1.3081, 1.4186, 1.399, 1.3978, 1.3814, 1.4091 and 1.4113 Å. Corresponding values are reported as 1.2753, 1.3492, 1.359, 1.3768, 1.3879, 1.3784, 1.3892 Å [36] and 1.2727, 1.347, 1.3594, 1.3884, 1.3777, 1.3776, 1.3903 Å [34]. In our previous work, the corresponding reported values are 1.27, 1.3456, 1.3566, 1.3872, 1.37, 1.3854 and 1.3827 Å [35]. The bond lengths C_4—O_{13}, C_3—N_{14}, N_{14}—C_{15}, C_{15}—O_{13} and C_3—C_4 are found to be 1.3436, 1.3739, 1.3001, 1.3804 and 1.3827 Å for mercaptobenzoxazole [11].

The CC bond lengths in ring I lie between 1.3897 and 1.4057 Å and in ring II lies between 1.3814 and 1.4091 Å. The

Table 2
Vibrational assignments of 2-(p-Fluorobenzyl)-6-nitrobenzoxazole.

HF/6-31G*			B3LYP/6-31G*			IR	Raman	SERS	Assignments[a]
υ(cm^{-1})	I_{IR}	R_A	υ(cm^{-1})	I_{IR}	R_A	υ(cm^{-1})	υ(cm^{-1})	υ(cm^{-1})	
3083	12.98	42.13	3155	8.74	48.73	–	–	–	υCHII(99)
3071	3.08	90.10	3142	2.30	96.90	–	–	–	υCHII(99)
3051	0.96	66.96	3122	1.65	74.41	–	–	–	υCHII(99)
3047	1.99	187.36	3120	3.32	202.86	–	–	–	υCHI(93)
3046	2.29	61.24	3119	2.86	67.96	3106	3104	–	υCHI(95)
3015	7.09	47.08	3085	4.98	36.03	–	–	–	υCHI(93)
3009	5.55	42.83	3084	7.77	55.54	–	3084	–	υCHI(95)
2941	1.80	57.76	3009	1.89	64.97	–	3011	2986	$\upsilon_{as}CH_2$(99)
2886	8.48	114.03	2959	8.00	139.65	–	2918	2933	υ_sCH_2(99)
1633	9.81	87.52	1609	10.34	214.86	1659	1620	1624	υPhII(61)
1625	33.00	44.11	1603	27.27	99.97	1605	–	–	υPhI(57) δCCCI(10)
1618	15.55	127.22	1596	6.96	96.12	–	–	–	υPhII(68)
1605	7.94	11.98	1589	5.32	9.19	1566	1566	1567	υPhI(83)
1583	239.16	265.58	1536	119.86	468.49	1523	1522	–	υC=N(69)
1518	114.27	1.51	1506	107.65	8.28	1511	–	–	δCHI(22) υPhI(64)
1476	51.85	9.99	1458	17.88	5.64	1463	1467	–	δCHII(23) υPhII(66)
1461	19.62	23.82	1456	19.58	33.88	–	–	1452	δCH_2(93)
1452	227.37	3.00	1429	106.96	20.85	1435	1435	–	δCHII(10) υPhII(24) $\upsilon_{as}NO_2$(60)
1417	2.90	0.24	1413	1.50	1.15	1416	1415	–	υPhI(61) δCHI(26)
1400	119.29	10.74	1405	18.25	46.04	–	–	–	υPhII(76)
1333	14.18	6.27	1363	62.18	49.72	1368	1367	1343	υPhII(22) υ_sNO_2(70)
1322	4.18	9.05	1335	0.42	10.46	1344	1341	–	δCH_2(45) υPhI(35) δCHI(13)
1318 δCHI(42)	417.36	404.91	1310	1.79	1.71	1308	1309	–	υPhI(42)
1298	93.10	61.02	1304	0.29	5.54	–	–	–	υPhII(65)
1275	21.28	17.39	1261	9.81	9.50	1266	1266	1286	δCHII(54)
1258	18.33	8.67	1250	4.07	33.99	–	–	–	δCH_2(69)
1222	75.07	1.99	1233	482.41	754.29	–	1238	–	υC_6N_{10}(64) δNO_2(17)
1219	44.71	81.59	1218	77.37	17.25	1214	1216	1217	$\upsilon C_{25}F_{28}$(45) υPhI(19) δCCC(10) δCHI(17)
1218	28.33	21.68	1209	11.06	95.10	–	1194	–	υC_3N_{14}(49) υPhII(23) δCHII(15)
1184	8.17	9.06	1183	3.30	14.51	–	–	–	$\upsilon C_{16}C_{18}$(40) υPhI(18) δCHI(17)
1169	22.20	1.58	1165	22.62	8.81	1160	–	–	δCHI(67)
1165	12.24	4.32	1164	22.10	9.52	1142	1160	–	δCCCII(24) υC_4O_{13}(49) δCH_2(16)
1129	25.33	1.42	1121	46.33	28.62	–	1118	1124	δCHII(71)
1114	1.09	36.25	1107	7.50	18.20	–	–	–	δCHI(54) δCCCII(10) υPhI(15)
1094	3.51	3.13	1093	8.76	20.45	1095	–	1078	δCHII(70)
1057	13.08	47.13	1042	15.82	33.61	1056	1057	1044	δCHII(23) υPhII(47) υC_4O_{13}(11) υC_6N_{10}(15)
1041	0.13	2.05	1014	6.69	0.82	1016	–	1003	δCHI(64)
1023	0.05	0.11	981	0.65	1.41	–	–	–	γCHII(87)
1017	6.10	0.32	961	0.31	0.90	–	–	–	γCHI(83)
1008	1.02	1.66	951	0.42	1.12	951	–	–	δCH_2(12) γCHI(63) τCCCCI(13)
973	39.10	1.96	938	2.50	3.94	934	940	940	δCH_2(32) γCHI(62)
951	4.52	2.23	913	30.96	1.30	–	–	–	γCHII(77) τCCCCII(13)

Table 2 (*continued*)

HF/6-31G*			B3LYP/6-31G*			IR	Raman	SERS	Assignments[a]
$\upsilon(cm^{-1})$	I_{IR}	R_A	$\upsilon(cm^{-1})$	I_{IR}	R_A	$\upsilon(cm^{-1})$	$\upsilon(cm^{-1})$	$\upsilon(cm^{-1})$	
924	7.60	9.60	910	4.63	5.49	886	–	–	$\upsilon C_4O_{13}(17)$ $\delta CCCII(23)$ $\upsilon C_6N_{10}(11)$
893	36.29	1.74	852	15.53	5.29	859	860	878	$\upsilon O_{13}C_{15}(24)$ $\delta RingIII(22)$ $\upsilon C_{15}C_{16}(41)$
887	37.87	1.47	845	10.40	10.42	–	–	–	$\upsilon O_{13}C_{15}(32)$ $\gamma CHI(47)$
886	39.42	0.99	844	28.48	1.98	838	–	–	$\gamma CHII(78)$
866	0.22	2.66	829	13.36	32.72	–	832	831	$\delta CCCI(13)$ $\upsilon O_{13}C_{15}(13)$ $\upsilon PhI(58)$
837	37.82	12.73	824	2.49	4.15	820	–	–	$\gamma CHI(97)$
823	38.21	33.61	814	60.48	14.21	–	–	–	$\upsilon O_{13}C_{15}(13)$ $\gamma CHI(44)$
803	96.54	14.23	778	63.59	20.76	773	773	–	$\delta NO_2(72)$
784	4.96	6.01	764	18.49	10.86	–	763	752	$\tau CCCCI(17)$ $\gamma RingIII(13)$ $\delta CH_2(55)$ $\delta CCC(12)$
767	2.62	3.88	737	0.81	1.93	736	737	–	$\tau CCCCII(59)$ $\tau RingIII(24)$
724	12.32	2.39	722	4.96	3.16	–	–	–	$\delta RingIII(24)$ $\delta CCCI(21)$ $\upsilon C_{16}C_{18}(29)$
722	34.28	6.19	692	20.28	3.86	–	–	–	$\gamma NO_2(48)$ $\gamma CN(17)$
708	0.97	1.82	686	1.50	3.40	688	689	–	$\tau CCCCI(61)$ $\gamma CF(11)$
686	15.79	5.43	675	9.86	4.12	664	–	675	$\delta NO_2(23)$ $\delta CCCII(38)$ $\delta RingIII(31)$
653	14.56	5.49	648	7.58	6.73	–	650	–	$\tau RingIII(26)$ $\delta CCCI(10)$ $\gamma RingIII(13)$
642	0.66	6.15	637	1.48	5.58	–	633	607	$\delta CCCI(64)$
583	0.14	0.18	570	0.07	0.79	579	580	–	$\tau CCCCII(52)$ $\gamma CN(19)$ $\tau RingIII(11)$
569	5.22	5.95	562	1.35	9.34	551	548	556	$\delta CCCII(35)$ $\tau RingIII(33)$
536	6.93	0.21	533	4.05	0.56	522	528	522	$\delta NO_2(52)$ $\delta CCCII(23)$ $\delta CN(15)$
519	13.64	1.57	512	11.44	1.02	503	502	–	$\tau CCCCI(28)$ $\gamma CF(27)$ $\gamma CC_{16}(10)$ $\delta CCCI(10)$
485	12.00	2.32	478	8.39	3.73	–	–	498	$\tau CCCCI(24)$ $\gamma CF(23)$ $\delta CCCI(18)$
440	5.11	0.47	436	0.20	2.18	–	438	435	$\delta NO_2(20)$ $\delta RingIII(46)$ $\delta CCCII(15)$
434	4.25	3.74	427	5.20	0.99	426	–	–	$\tau CCCCII(62)$ $\tau RingIII(19)$
428	0.02	0.02	420	0.35	0.06	411	–	–	$\tau CCCCI(85)$
403	4.60	0.15	399	3.13	0.58	–	–	–	$\delta CF_{28}(56)$ $\delta CCCI(16)$ $\delta C_{19}C_{16}C_{18}(17)$
372	3.87	2.73	366	2.29	3.11	–	378	366	$\delta CCCI(31)$ $\delta CCCII(30)$
347	2.83	4.40	336	1.68	5.22	–	347	–	$\tau RingIII(20)$ $\gamma RingIII(13)$ $\gamma CN(11)$ $\gamma CC_{16}(10)$ $\tau CCCCII(12)$
315	0.56	2.70	318	0.62	2.06	–	323	–	$\delta CCCII(33)$ $\delta C_{20}C_{16}C_{18}(13)$ $\delta C_{19}C_{16}C_{18}(13)$
309	0.63	0.93	296	1.07	2.33	–	290	–	$\delta C_{20}C_{16}C_{18}(19)$ $\delta C_{19}C_{16}C_{18}(19)$ $\delta RingIII(15)$

(*continued on next page*)

Table 2 (*continued*)

HF/6-31G*			B3LYP/6-31G*			IR	Raman	SERS	Assignments[a]
υ(cm^{-1})	I_{IR}	R_A	υ(cm^{-1})	I_{IR}	R_A	υ(cm^{-1})	υ(cm^{-1})	υ(cm^{-1})	
280	0.46	1.12	274	0.15	1.26	–	260	–	τCCCCII(39) τRingIII(16) γCN(11)
246	7.47	1.27	243	4.18	0.94	–	–	–	δCN(28) $\delta C_{20}C_{16}C_{18}$(22) $\delta C_{19}C_{16}C_{18}$(22) δRingIII(14)
191	6.31	1.51	189	3.97	2.09	–	185	–	τCCCCI(12) δCH_2(12) $\delta C_{15}C_{18}C_{16}$(12) τCCCCII(11)
155	3.29	0.44	157	2.90	0.62	–	164	–	δCN(40) δRingIII(23)
130	2.36	0.43	125	1.51	0.37	–	124	–	τCCCCII(64)
86	0.60	0.51	86	0.58	0.44	–	100	–	τRingIII(30) γCN(31) τCCCCII(25)
52	0.10	0.24	61	0.09	0.21	–	–	–	τNO_2(81)
15	0.22	6.44	27	0.19	7.38	–	–	–	γRingIII(35) δCH_2(28) $\delta C_{15}C_{18}C_{16}$(28)
20	0.53	5.49	22	0.12	9.60	–	–	–	τCH_2(20) τRingIII(80)
27	0.13	10.17	11	0.34	8.69	–	–	–	τRingIII(84)

υ-stretching; δ-in-plane deformation; γ-out-of-plane deformation; τ-twisting; PhI-para substituted phenyl ring; PhII-ortho substituted phenyl ring; RingIII- benzoxazole

CH bond lengths in rings I and II lie respectively between 1.0829–1.0856 Å and 1.0803–1.0825 Å. Here for the title compound, benzene is a regular hexagon with bond lengths somewhere in between the normal values for a single (1.54 Å) and a double (1.33 Å) bond [52].

Purkayastha and Chattopadhyay [53] reported N_{14}=C_{15}, N_{14}—C_3 bond lengths as 1.3270, 1.400 Å for benzothiazole and 1.3503, 1.407 Å for benzimidazole compounds. Ambujakshan et al. has reported the same as 1.2753 and 1.3892 Å [36]. In the present case, the respective bond lengths are 1.3081 and 1.4113 Å. In our previous work [35], the corresponding values are obtained as 1.2700 and 1.3827 Å. The bond lengths C—F is reported as 1.3242 [35], 1.3267 Å [34] and in the present case as 1.3915 Å. Theoretical calculations give shortening of the angles C_1—C_6—C_{10} and C_5—C_6—C_{10} by 1.5° and 2.1° from 120° at C_6 position respectively and C_6—N_{10}—O_{11} and C_6—N_{10}—O_{12} by 2° and 1.8° from 120° at N_{10} position respectively.

The highly electronegative fluorine atom tries to obtain additional electron density and it attempts to draw electrons from the neighboring atoms. The neighboring H atoms move closer to F in order to share the electrons more easily. This resulted in an increase of C21—C25—C23 angle by 2.5°. This has been reported as 122.5° [35] and 122.4° [34] and the values are in good agreement with the present value.

The benzoxazole moiety is nearly planar with respect to the phenyl ring II which is evident from the torsion angles C_6—C_5—C_4—O_{13} = −179.8°, C_5—C_4—O_{13}—C_{15} = 179.7°, C_1—C_2—C_3—N_{14} = 179.8° and C_2—C_3—N_{14}—C_{15} = −179.8° whereas tilted from ring I which is evident from the torsion angles C_{18}—C_{16}—C_{15}—O_{13} = −77.5° and C_{18}—C_{16}—C_{15}—N_{14} = 100.1°. At C_4, C_5—C_4—O_{13} is increased by 8.7°, C_3—C_4—O_{13} is reduced by 12.6° and at C_3 position, C_4—C_3—N_{14} is decreased by 11.1°, C_2—C_3—N_{14} is increased by 10.9° from 120°, which shows the interaction between the benzoxazole moiety and phenyl ring II. At C_{15}, the bond angles O_{13}—C_{15}—C_{16}, O_{13}—C_{15}—N_{14} and C_{14}—C_{15}—N_{16} are 117°, 113.8° and 129.1° respectively. The asymmetry of these angles reveals the interaction between the methylene moiety and O_{13}.Nonlinear optics deals with the interaction of applied electromagnetic fields in various materials to generate new electromagnetic fields, altered in wavenumber, phase, or other physical properties [17]. Organic molecules able to manipulate photonic signals efficiently are of importance in technologies such as optical communication, optical computing, and dynamic image processing [18,19]. In this context, the dynamic first hyperpolarizability of the title compound is also calculated in the present study. The first hyperpolarizability (β_0) of this novel molecular system is calculated using B3LYP method, based on the finite field approach. In the presence of an applied electric field, the energy of a system is a function of the electric field. First hyperpolarizability is a third rank tensor that can be described by a $3 \times 3 \times 3$ matrix. The 27 components of the 3D matrix can be reduced to 10 components due to the Kleinman symmetry [54]. The components of β are defined as the coefficients in the Taylor series expansion of the energy in the external electric field. When the electric field is weak and homogeneous, this expansion becomes

$$E = E_0 - \sum_i \mu_i F^i - \frac{1}{2}\sum_{ij} \alpha_{ij} F^i F^j - \frac{1}{6}\sum_{ijk} \beta_{ijk} F^i F^j F^k - \frac{1}{24} \times \sum_{ijkl} \gamma_{ijkl} F^i F^j F^k F^l + \ldots$$

where E_0 is the energy of the unperturbed molecule, F^i is the field at the origin, μ_i, α_{ij}, β_{ijk} and γ_{ijkl} are the components of dipole moment, polarizability, the first hyperpolarizabilities, and second hyperpolarizibilites, respectively. The calculated first hyperpolarizability of the title compound is 17.7×10^{-30} esu, which comparable with the reported values of similar derivatives [55] and which is 136.15 times that of the standard NLO material urea (0.13×10^{-30} esu) [56]. We conclude that the title compound is an attractive object for future studies of nonlinear optical properties.

In order to investigate the performance, root mean square (RMS) value between calculated and observed wavenumbers were calculated. RMS values of the wavenumbers were evaluated using the following expression [57]. $\mathrm{RMS} = \sqrt{\frac{1}{n-1}\sum_i^n (\upsilon_i^{calc} - \upsilon_i^{exp})^2}$. The RMS error of the observed Raman and IR bands are found to be 27.35, 28.34 for HF and 10.70, 12.90 for B3LYP methods, respectively. The small differences between experimental and calculated vibrational modes are observed. This is due to the fact that

experimental results belong to solid phase and theoretical calculations belong to gaseous phase.

4.3. SERS spectrum

The relative intensities of the bands from the SERS spectra are expected to differ significantly from those of normal Raman spectrum owing to specific selection rules [58]. Surface selection rules suggest that, for a molecule adsorbed flat on the silver surface, its out-of-plane bending modes will be more enhanced when compared to its in-plane bending modes, and vice versa when it is adsorbed perpendicular to the silver surface [59]. It is further seen that vibrations involving atoms that are closer to the silver surface will be more enhanced. In the present study, the CH_2 stretching modes attached to the phenyl ring PhI appear at 2986 and 2933 cm^{-1} in the SERS spectrum. It should be related to the closeness of the CH_2 group to the metal surface. This is justifiable because the modes in groups directly interacting with the metal surface will be prominent in the SERS spectrum and undergo a wavenumber shift [60]. Further the CH_2 bands at 1452, 752 cm^{-1} and C_{15}—C_{16} stretching mode at 878 cm^{-1} are also observed in the SERS spectrum thereby supporting the above argument. Bunding et al. [61] noticed a significant shift and broadening of the methyl modes in the SERS spectrum in the case of 2-methylpyridine. They explained this in terms of the interaction of the methyl group and the metal surface. In the case of the SERS spectrum of β-hydroxyl-β-methylbutanoic acid, the bands corresponding to CH_2 and CH_3 modes at 1447, 880, 725 and 692 cm^{-1} suggest that these moieties assist the molecule to bind to the silver surface [62]. In the SERS study of (RS)-phenylsuccinic acid, the CH_2 stretching mode is observed at 2920 cm^{-1} and downshifted from the normal Raman spectrum by 24 cm^{-1} [63]. For, L-histidine the CH_2 stretching mode is downshifted from 2968 to 2933 cm^{-1} in the SERS spectrum in silver colloid [64]. For 2-phenoxymethylbenzothiazole, the $\upsilon_{as}CH_2$ mode was reported at 2953 cm^{-1} in the SERS spectrum which indicated the closeness of CH_2 group with metal surface and interaction of the silver surface with phenoxy group [65].

For the title compound the symmetric stretching mode of NO_2 seen at 1367 cm^{-1} in the normal Raman spectrum is observed at 1343 cm^{-1} in the SERS spectrum. The downshift of NO_2 may be due to the charge transfer from the oxygen atoms of the nitro group to the metal [66–68]. According to surface selection rule, the vibrations involving atoms that are close to the metal surface will be enhanced [58,59]. Interaction through the NO_2 group was also supported by the presence of modes at 675, 522 and 435 cm^{-1}. For 2-amino-5-nitropyrimidine [66] the symmetric NO_2 stretching mode corresponds to the most intense band, which appears broad and significantly downshifted from 1344 cm^{-1} (Raman) to 1326 cm^{-1} (SERS), suggesting a binding to silver surface through the lone pairs of oxygen atom. Carasco et al. [67] observed NO_2 stretching band in the SERS spectrum at around 1500 cm^{-1} with medium intensity which demonstrates the importance of nitro group in regard to the interaction with the metal. Further, they observed the enhancement of phenyl ring modes revealing that the molecule is oriented perpendicular to the metal surface where as the changes that occur in the nitro group indicates that the interaction occurs through O atoms of the nitro moiety. The interaction induces a π electronic redistribution primarily around both the nitro group and the aromatic portion in the vicinity of the substituent site. Also Gao and Weaver [68] observed broadening and downshift of the corresponding band of nitrobenzene, adsorbed on gold via nitro group.

The CH stretching vibrations of the benzene ring, in the region 3000–3100 cm^{-1} has been shown to be an unambiguous probe in the determination of surface orientation of substituted aromatics [69]. Since CH stretching modes do not mix significantly with other vibrational modes of the aromatic ring, their SERS intensities are known to provide the most specific evidence of the orientation of the adsorbate with respect to the surface [70]. The presence or absence of the benzene ring CH stretching vibration is a reliable probe for the perpendicular or parallel orientation, respectively, of the benzene ring with respect to the surface [71,72]. Hence, in the present case the complete absence of the CH stretching bands in the SERS spectrum means that the adsorbed molecule may lie flat on the metal surface. With a flat orientation, the benzene rings may also interact with the metal surface directly.

For the phenyl ring I, the υPh modes are observed in the SERS spectrum at 1567, 1217 and 831 cm^{-1} without any significant shift from the normal Raman values. Also the in-plane and out-of-plane CH modes of the ring PhI are observed at 1003 and 940 cm^{-1} in the SERS spectrum. For the phenyl ring PhII, the ring stretching modes are observed in the SERS spectrum at 1624, 1044 cm^{-1}. For the ring PhII, the ring breathing mode is observed at 1057 cm^{-1} in the normal Raman spectrum and this band is redshifted by 13 cm^{-1} in the SERS spectrum with significant band broadening. It has been documented in literature [73], that when a benzene ring moiety interacts directly with a metal surface, the ring breathing mode is red shifted by 10 cm^{-1} along with substantial band broadening in the SERS spectrum. In the present case no such shift was observed for phenyl ring PhI, but in the case of PhII, such a shift was observed, which shows the direct interaction of the benzene ring Ph II and the metal surface. The in-plane CH bending modes of phenyl ring PhII are observed at 1286, 1124 and 1078 cm^{-1} in the SERS spectrum. It may be inferred that the phenyl ring PhI is more tilted from the metal surface due to the presence of in-plane and out-of-plane CH bending modes, in-plane ring deformation bands at 607 and 498 cm^{-1}. But for the phenyl ring PhII, out-of-plane CH bands are absent in the SERS spectrum, while the in-plane CH bending modes and in-plane ring deformations bands (556, 435 cm^{-1}) are present in the SERS spectrum, which suggest a nearly perpendicular orientation with respect to the metal surface.

5. Conclusion

The FT-Raman and FT-IR spectra of 2-(p-Fluorobenzyl)-6-nitrobenzoxazole were recorded and analyzed. The surface enhanced Raman scattering (SERS) spectrum was recorded in a silver colloid. The molecular geometry and wavenumbers were calculated theoretically using Gaussian03 software package. The observed wavenumbers were found to be in agreement with calculated (B3LYP) values. Optimized geometrical parameters of the title compound are in agreement with the reported values. From a comparison of SERS and normal Raman spectra, it can be deduced that the title compound is adsorbed on the metal surface and that it interacts with the silver sol via CH_2 and NO_2 groups. The SERS study reveals a tilted orientation for the para substituted phenyl ring and a nearly perpendicular orientation for the tri-substituted phenyl ring with respect to the metal surface. The predicted infrared intensities, Raman activities and first hyperpolarizability values are reported.

Acknowledgments

Sheena Mary Y. would like to thank University Grants Commission, India, for a research fellowship and Dr. Hema Tresa Varghese, Associate Professor, Department of Physics, Fatima Mata National College, Kollam, Kerala, India, for providing computational facility.

References

[1] O. Temiz-Arpaci, I. Oren, N. Altanlar, II Farmaco 57 (2002) 175.
[2] I. Yildiz-Oren, I. Yalcin, E. Aki-Sener, N. Ucarturk, Eur. J. Med. Chem. 39 (2004) 291.
[3] O. Temiz-Arpaci, A. Ozdemir, I. Yalcin, I. Yildiz, E. Aki-Sener, N. Altanlar, Arch. Pharm. 338 (2005) 105.

[4] O. Temiz-Arpaci, B. Tekiner-Gulbas, I. Yildiz, E. Aki-Sener, I. Yalcin, Bioorg. Med. Chem. 13 (2005) 6354.
[5] H. Lage, E. Aki-Sener, I. Yalcin, Int. J. Cancer 119 (2006) 213.
[6] S. Lochrunner, K. Stock, E. Riedle, J. Mol. Struct. 700 (2004) 13.
[7] J. Catalan, P. Perez, J.C. Valle, J.L.G. Paz, M. Kasha, Proc. Natl. Acad. Sci. USA 101 (2004) 419.
[8] C. Tanner, C. Manca, S. Leutwyler, Science 302 (2003) 1736.
[9] A. Akbay, A.I. Oren, O. Temiz-Arpaci, E. Aki-Sener, I. Yalcin, Arzneim. Forsch. Drug Res. 53 (2003) 266.
[10] E. Aki-Sener, O. Temiz-Arpaci, I. Yalcin, N. Altanlar, Il Farmaco 55 (2002) 397.
[11] A. Bigotto, B. Pergolese, J. Raman Spectrosc. 32 (2001) 953.
[12] R. Cristiano, A.A. Vieira, F. Ely, H. Gallardo, Liq. Cryst. 33 (2006) 381.
[13] R. Cristiano, D.M.P.O. Santos, G. Conte, H. Gallardo, Liq. Cryst. 33 (2006) 997.
[14] C.S. Wang, I.W. Wang, K.L. Chen, C.K. Lai, Tetrahedron 62 (2006) 9383.
[15] U.V. Vasconcelos, E. Dalmolin, A.A. Merio, Org. Lett. 7 (2005) 1027.
[16] E. Tasal, I. Sidir, Y. Gulseven, C. Ogretir, T. Onkol, J. Mol. Struct. 923 (2009) 141.
[17] Y.R. Shen, The Principles of Nonlinear Optics, Wiley, New York, 1984.
[18] P.V. Kolinksy, Opt. Eng. 31 (1992) 1676.
[19] D.F. Eaton, Science 253 (1991) 281.
[20] C.R. Moylan, R.J. Twieg, V.Y. Lee, S.A. Swanson, K.M. Betterton, R.D. Miller, J. Am. Chem. Soc. 115 (1993) 12599.
[21] S. Gilmour, R.A. Montigomery, S.R. Marder, L.T. Cheng, A.K.Y. Jen, Y. Cai, J.W. Perry, L.R. Dalton, Chem. Mater. 6 (1994) 1603.
[22] Y.S. Mary, C.Y. Panicker, H.T. Varghese, K. Raju, T.E. Bolelli, I. Yildiz, C.M. Granadeiro, H.I.S. Nogueira, J. Mol. Struct. 994 (2011) 223.
[23] T. Ertan, I. Yildiz, B. Tekiner-Gulbas, K. Bolelli, O. Temiz-Arpaci, S. Ozkan, F. Kaynak, I. Yalcin, E. Aki, Eur. J. Med. Chem. 44 (2009) 501.
[24] P.C. Lee, D.J. Meisel, J. Phys. Chem. 86 (1982) 3391.
[25] M.J. Frisch, G.W. Trucks, H.B. Schlegel, G.E. Scuseria, M.A. Robb, J.R. Cheeseman, J.A. Montgomery Jr., T. Vreven, K.N. Kudin, J.C. Burant, J.M. Millam, S.S. Iyengar, J. Tomasi, V. Barone, B. Mennucci, M. Cossi, G. Scalmani, N. Rega, G.A. Petersson, H. Nakatsuji, M. Hada, M. Ehara, K. Toyota, R. Fukuda, J. Hasegawa, M. Ishida, T. Nakajima, Y. Honda, O. Kitao, H. Nakai, M. Klene, X. Li, J.E. Knox, H.P. Hratchian, J.B. Cross, C. Adamo, J. Jaramillo, R. Gomperts, R.E. Stratmann, O. Yazyev, A.J. Austin, R. Cammi, C. Pomelli, J.W. Ochterski, P.Y. Ayala, K. Morokuma, G.A. Voth, P. Salvador, J.J. Dannenberg, V.G. Zakrzewski, S. Dapprich, A.D. Daniels, M.C. Strain, O. Farkas, D.K. Malick, A.D. Rabuck, K. Raghavachari, J.B. Foresman, J.V. Ortiz, Q. Cui, A.G. Baboul, S. Clifford, J. Cioslowski, B.B. Stefanov, G. Liu, A. Liashenko, P. Piskorz, I. Komaromi, R.L. Martin, D.J. Fox, T. Keith, M.A. Al-Laham, C.Y. Peng, A. Nanayakkara, M. Challacombe, P.M.W. Gill, B. Johnson, W. Chen, M.W. Wong, C. Gonzalez, J.A. Pople, Gaussian 03, Revision C. 02 Gaussian, Inc, Wallingford CT, 2004.
[26] J.B. Foresman, in: E. Frisch (Ed.), Exploring Chemistry with Electronic Structure Methods: A Guide to Using Gaussian, Gaussian, Pittsburg, PA, 1996.
[27] A.P. Scott, L. Radom, J. Phys. Chem. 100 (1996) 16502.
[28] G. Rauhut, P. Pulay, J. Phys. Chem. 99 (1995) 3093.
[29] J.M.L. Martin, C. Van Alsenoy, GAR2PED Program, University of Antwerpen, Belgium, 1995.
[30] N.G.P. Roeges, A Guide to the Complete Interpretation of the Infrared spectra of organic structures, Wiley, NewYork, 1994.
[31] C.Y. Panicker, H.T. Varghese, L. Usha Kumari, T. Ertan, I. Yildiz, C.M. Granadeiro, H.I.S. Nogueira, Y.S. Mary, J. Raman Spectrosc. 41 (2010) 381.
[32] N. Sundaraganesan, S. Ayyappan, H. Umamaheshawari, B.D. Joshua, Spectrochim. Acta 66A (2007) 17.
[33] N.B. Colthup, L.H. Daly, S.E. Wiberly, Introduction to Infrared and Raman Spectroscopy, third ed., Academic Press, Boston, 1990.
[34] P.L. Anto, C.Y. Panicker, H.T. Varghese, D. Philip, O. Temiz-Arpaci, B. Tekiner-Gulbar, I. Yildiz, Spectrochim. Acta Part A 67 (2007) 744.
[35] Y.S. Mary, H.T. Varghese, C.Y. Panicker, T. Ertan, I. Yildiz, O. Temiz-Arpaci, Spectrochim. Acta 71A (2008) 566.
[36] K.R. Ambujakshan, V.S. Madhavan, H.T. Varghese, C.Y. Panicker, O. Temiz-Arpaci, B. Tekiner-Gulbas, I. Yildiz, Spectrochim. Acta 69A (2008) 782.
[37] I. Yalcin, E. Sener, T. Ozden, S. Ozden, A. Akin, Eur. J. Med. Chem. 25 (1990) 705.
[38] R. Saxena, L.D. Kandpal, G.N. Mathur, J. Polym. Sci. Part A: Polym. Chem. 40 (2002) 3959.
[39] R.M. Silverstein, G.C. Bassler, T.C. Morril, Spectrometric Identification of Organic Compounds, fifth ed., John Wiley and Sons Inc., Singapore, 1991.
[40] K. Nakamoto, Infrared and Raman Spectrum of Inorganic and Coordination Compounds, fifth ed., John Wiley and Sons Inc., Singapore, 1997.
[41] T.D. Klots, W.B. Collier, Spectrochim. Acta 51A (1995) 1291.
[42] P. Sett, N. Paul, S. Chattopadhyay, P.K. Mallick, J. Raman Spectrosc. 30 (1999) 277.
[43] P. Sett, S. Chattopadhyay, P.K. Mallick, Spectrochim. Acta 56A (2000) 855.
[44] P. Sett, S. Chattopadhyay, P.K. Mallick, J. Raman Spectrosc. 31 (2000) 177.
[45] V. Volovsek, G. Baranovic, L. Colombo, J.R. Durig, J. Raman Spectrosc. 22 (1991) 35.
[46] M. Muniz-Miranda, E. Castelluci, N. Neto, G. Sbrana, Spectrochim, Acta 39A (1983) 107.
[47] G. Varsanyi, Assignments of Vibrational Spectra of Seven Hundred Benzene Derivatives, Wiley, New York, 1974.
[48] C.Y. Panicker, K.R. Ambujakshan, H.T. Varghese, S. Mathew, S. Ganguli, A.K. Nanda, C. Van Alsenoy, J. Raman Spectrosc. 40 (2009) 527.
[49] V.S. Madhavan, H.T. Varghese, S. Mathew, J. Vinsova, C.Y. Panicker, Spectrochim. Acta 72A (2009) 547.
[50] G. Socrates, Infrared Characteristic Group Frequencies, Wiley-Interscience, New York, 1980.
[51] A. Lifshitz, C. Tamburu, A. Suslensky, F. Dubnikova, J. Phys. Chem. A 110 (2006) 4617.
[52] P. Sykes, A Guide Book to Mechanism in Organic Chemistry, sixth ed., Pearson Education, India, 2004.
[53] P. Purkayastha, N. Chattopadhyay, Phys. Chem. Chem. Phys. 2 (2003) 303.
[54] D.A. Kleinman, Phys. Rev. 126 (1962) 1977.
[55] L.N. Kuleshova, M.Y. Antipin, V.N. Khrustalev, D.V. Gusev, E.S. Bobrikova, Kristallografiya 48 (2003) 645.
[56] M. Adant, L. Dupuis, L. Bredas, Int. J. Quantum. Chem. 56 (2004) 497.
[57] L. Ushakumari, H.T. Varghese, C.Y. Panicker, T. Ertan, I. Yildiz, J. Raman Spectrosc. 39 (2008) 1832.
[58] J.A. Creighton, Spectroscopy of Surfaces – Advances in Spectroscopy, vol. 16, Wiley, New York, 1988. p. 37 (Chapter 2).
[59] X. Gao, J.P. Davies, M.J. Weaver, J. Phys. Chem. 94 (1990) 6858.
[60] S. Kai, W. Chaozhi, X. Guangzhi, Spectrochim. Acta 45A (1989) 1029.
[61] K.A. Bunding, J.R. Lombardi, R.L. Birke, Chem. Phys. 49 (1980) 53.
[62] E. Podstawka, M. Swiatlowska, E. Borowiec, L.M. Proniewicz, J. Raman Spectrosc. 38 (2007) 356.
[63] D. Sajan, A. Fischer, I.H. Joe, V.S. Jayakumar, Spectrochim. Acta 64A (2006) 580.
[64] J.K. Lim, Y. Kim, S.Y. Lee, S.W. Joo, Spectrochim. Acta 69A (2008) 286.
[65] C.Y. Panicker, H.T. Varghese, A. Raj, K. Raju, T. Ertan-Bolelli, I. Yildiz, O. Temiz-Arpaci, C.M. Granadeiro, H.I.S. Nogueira, Spectrochim. Acta 74A (2009) 132.
[66] M. Muniz-Miranda, Vib. Spectrosc. 29 (2002) 229.
[67] E.A. Carasco, F.M. Campos-Vallette, P. Leyton, G. Diazf, R.E. Clavijo, J.V. Garcia-Ramos, N. Inostroza, C. Domingo, S. Sanchez-Cortes, R. Koch, J. Phys. Chem. 107 (2003) 9611.
[68] P. Gao, M.J. Weaver, J. Phys. Chem. 89 (1985) 5040.
[69] Y.J. Kwon, D.H. Son, S.J. Ahn, M.S. Kim, K. Kim, J. Phys. Chem. 98 (1994) 8481.
[70] M. Moskovits, J.S. Suh, J. Phys. Chem. 92 (1988) 6327.
[71] J.S. Suh, M. Moskovits, J. Am. Chem. Soc. 108 (1986) 4711.
[72] J.A. Creighton, Surf. Sci. 124 (1983) 209.
[73] P. Cao, M.J. Weaver, J. Phys. Chem. 93A (1989) 6205.